

Geophysical Research Letters°



RESEARCH LETTER

10.1029/2022GL101690

Key Points:

- Tropopause folding is much more frequent at higher reanalysis resolution, due almost entirely to vertical resolution
- Nearly 90% of folding in ERA5 (nearly 100% of Deep folding) is unrepresented in CAMSRA (at the resolution of ERA-Interim)
- Higher-resolution folding is more strongly correlated with tropospheric ozone, driven by deeper and more filamentary folding

Supporting Information:

Supporting Information may be found in the online version of this article.

Correspondence to:

S. Bartusek, samuel.bartusek@columbia.edu

Citation:

Bartusek, S., Wu, Y., Ting, M., Zheng, C., Fiore, A., Sprenger, M., & Flemming, J. (2023). Higher-resolution tropopause folding accounts for more stratospheric ozone intrusions. *Geophysical Research Letters*, 50, e2022GL101690. https://doi.org/10.1029/2022GL101690

Received 13 OCT 2022 Accepted 19 MAR 2023

Author Contributions:

Yutian Wu, Mingfang Ting, Cheng Zheng, Arlene Fiore Data curation: Samuel Bartusek, Johannes Flemming Formal analysis: Samuel Bartusek Funding acquisition: Yutian Wu, Mingfang Ting

Conceptualization: Samuel Bartusek,

Investigation: Samuel Bartusek Methodology: Samuel Bartusek, Yutian Wu, Mingfang Ting, Cheng Zheng, Arlene Fiore, Michael Sprenger, Johannes

Software: Samuel Bartusek, Michael Sprenger, Johannes Flemming

© 2023. The Authors.

This is an open access article under the terms of the Creative Commons Attribution License, which permits use, distribution and reproduction in any medium, provided the original work is properly cited.

Higher-Resolution Tropopause Folding Accounts for More Stratospheric Ozone Intrusions

Samuel Bartusek^{1,2} , Yutian Wu¹, Mingfang Ting^{1,2}, Cheng Zheng¹, Arlene Fiore³, Michael Sprenger⁴, and Johannes Flemming⁵

¹Lamont-Doherty Earth Observatory, Columbia University, Palisades, NY, USA, ²Department of Earth and Environmental Sciences, Columbia University, New York, NY, USA, ³Department of Earth, Atmospheric, and Planetary Sciences, Massachusetts Institute of Technology, Cambridge, MA, USA, ⁴Institute for Atmosphere and Climate Science, ETH Zürich, Zürich, Switzerland, ⁵European Centre for Medium-Range Weather Forecasts (ECMWF), Reading, UK

Abstract Ozone in the troposphere is a pollutant and greenhouse gas, and it is crucial to better understand its transport from the ozone-rich stratosphere. Tropopause folding, wherein stratospheric air intrudes downward into the troposphere, enables stratosphere-to-troposphere ozone transport (STT). However, systematic analysis of the relationship between folding and tropospheric ozone, using data that can both capture folding's spatial scales and accurately represent tropospheric chemistry, is limited. Here, we compare folding in high-resolution reanalysis ERA5 (0.25° horizontal, <21 hPa vertical) and low-resolution chemical reanalysis CAMSRA (0.75°, <40 hPa), against CAMSRA ozone, over 1 year. Folding becomes dramatically more frequent at high resolution, with vertical resolution overwhelmingly responsible. Deeper, more filamentary folding is almost entirely unrepresented at low resolution. Higher-resolution folding is better-correlated with tropospheric ozone (especially along midlatitude storm tracks, where deep folding is most common); STT is therefore likely more attributable to tropopause folding than coarsely-resolved folding can capture.

Plain Language Summary "Tropopause folding" refers to high-altitude atmospheric events wherein the "tropopause" (the boundary separating the troposphere, the lowest atmospheric layer, from the stratosphere above it) is perturbed, "folding" downward and allowing stratospheric air to intrude into the troposphere. These intrusions enable stratosphere-to-troposphere transport (STT) of ozone, a pollutant and greenhouse gas in the troposphere—however, a thorough understanding of the relationship between folding and ozone STT has been limited due to the difficulty of combining global yet detailed meteorological data with high-fidelity chemical data. Here, we identify folding occurrences in both high- and low-resolution representations of atmospheric motion throughout 1 year, and assess how strongly each folding data set is related to estimated tropospheric ozone. A high-resolution view reveals that folding events are much more frequent and widespread—and penetrate further into the troposphere, becoming thinner—than possible to represent at lower resolution. Moreover, folding at higher resolution is more closely correlated with nearby tropospheric ozone amounts. Folding may therefore exert influence over a larger proportion of ozone STT than is suggested by coarse representations of folding. Furthermore, our results identify the importance of vertical (rather than horizontal) resolution in representing such features and atmospheric transport.

1. Introduction

Ozone in the stratosphere is beneficial to life on earth, but in the troposphere (where it is much rarer) it is a pollutant hazardous to human health and crops (Krzyzanowski & Cohen, 2008; Monks et al., 2015) and an effective greenhouse gas (Myhre et al., 2013). Understanding the sources of tropospheric ozone is thus societally and climatically important. While photochemical production is the largest source of tropospheric ozone, stratosphere-to-troposphere transport (STT) is a significant contributor (Hess et al., 2015; Neu et al., 2014; Williams et al., 2019), and stratospheric influence on tropospheric ozone is projected to strengthen due both to global-warming-related changes in the stratospheric circulation and to stratospheric ozone recovery (Akritidis et al., 2019; Banerjee et al., 2016; Fu & Tian, 2019; Hegglin & Shepherd, 2009; Hess et al., 2015; Meul et al., 2018).

The dominant mechanism for STT of air is tropopause folding (Stohl et al., 2003), wherein an intrusion of the stratosphere into the troposphere allows exchange between the two layers, typically influencing upper- and

BARTUSEK ET AL. 1 of 11

Visualization: Samuel Bartusek Writing – original draft: Samuel Bartusek

Writing – review & editing: Samuel Bartusek, Yutian Wu, Mingfang Ting, Cheng Zheng, Arlene Fiore, Michael Sprenger, Johannes Flemming mid-tropospheric ozone concentrations (Danielsen, 1968; Shapiro, 1980). Folding can also enable large stratospheric influence on near-surface ozone in some regions—notably the eastern Mediterranean and Middle East (Akritidis et al., 2016; Tyrlis et al., 2014; Zanis et al., 2014), western United States (Langford et al., 1996, 2009; Langford & Reid, 1998; Lefohn et al., 2012; Wang et al., 2020), and Tibetan Plateau (X. L. Chen et al., 2011; X. Chen et al., 2013; Skerlak et al., 2019). But a more precise and systematic assessment of folding's role in ozone STT and relationship to tropospheric ozone than established by previous global studies (Beekmann et al., 1997; Boothe & Homeyer, 2017; Skerlak et al., 2014; Sprenger & Wernli, 2003) is possible due to new analysis tools.

Gaps in understanding the relationships between tropopause folding, ozone STT, and tropospheric ozone have persisted due to limitations in both meteorological and chemical data. First, global-scale analyses of folding and its role in STT (Akritidis et al., 2019; Skerlak et al., 2015; Sprenger et al., 2003) have been restricted by available reanalysis resolution (recently extended to 50 km horizontally; Akritidis et al., 2021). Capturing fold morphology and fold-related turbulent STT processes is known to require resolution of at least 50 km (Buker et al., 2005; Knowland, Ott, et al., 2017; Spreitzer et al., 2019), but whether such resolutions are sufficient remains unknown, as does any estimation of necessary vertical resolution. In ERA5, currently the highest horizontal and vertical resolution reanalysis, "double-tropopause" structures (of which folding is one type) are significantly more frequent than in ERA-Interim (Hoffmann & Spang, 2022), but no systematic analysis of folding in ERA5 has been conducted. High-resolution observational evidence, although sparse and localized, has suggested that atmospheric transport structures are horizontally and vertically filamentary, characterized by thin, diffusion-resistant layers (Appenzeller & Davies, 1992; Appenzeller et al., 1996; Danielsen, 1959; Newell et al., 1996, 1999; Trickl et al., 2010, 2020). Resolution, both horizontal and vertical, may therefore greatly impact the representation of tropopause folding and its associated transport (Akritidis et al., 2021). Second, the fidelity of reanalysis ozone (particularly tropospheric) is constrained by both observational sparseness and, crucially, a lack of integrated chemical transport models (Dragani, 2010; Knowland, Ott, et al., 2017; Park et al., 2020; Wargan et al., 2017). Therefore, despite reanalysis- and observation-based research on folding and its STT and ozone impacts (largely separately), a systematic global-scale relation of tropospheric ozone to tropopause folding has remained elusive.

Characterization of tropopause folding and its relationship with tropospheric ozone therefore lacks both (a) analysis of folding in a global data set of sufficient meteorological fidelity, and (b) analysis of its ozone impacts in a global data set of sufficient chemical fidelity. Here, addressing both gaps, we identify folding throughout 1 year in both high-resolution reanalysis ERA5 and a lower-resolution chemical reanalysis CAMSRA (with meteorology assimilated nearly-identically to ERA5 but at the resolution of ERA-Interim), and assess the relationship between both folding datasets and tropospheric ozone (derived from CAMSRA). Specifically, we address the following questions:

- 1. How are frequencies and global distributions of folding affected by reanalysis resolution, and what are the roles of horizontal versus vertical resolution?
- 2. How is the relationship between folding and tropospheric ozone affected by folding resolution?
- 3. How may folding frequency or morphology differences account for differing folding-ozone relationships?
- 4. What do our findings imply about ozone STT associated with folding?

2. Data and Methods

We analyze data throughout 2012 from reanalyses CAMSRA (Copernicus Atmosphere Monitoring Service Reanalysis; European Center for Medium-range Weather Forecasting [ECMWF]) and ERA5 (ECMWF Reanalysis version 5). CAMSRA (Inness et al., 2019) is a new chemical reanalysis at T255 spectral horizontal resolution (0.75°, 79 km grid) and 60 vertical levels to 0.1 hPa. ERA5 (Hersbach et al., 2020) is the latest ECMWF meteorological reanalysis at T639 resolution (0.25°, 31 km) and 137 levels to 0.01 hPa. Both reanalyses are produced by ECMWF's Integrated Forecasting System (IFS) using 4D-Var data assimilation; ERA5 uses IFS Cycle 41r2 and CAMSRA uses Cycle 42r1 (both implemented in 2016). CAMSRA meteorological fields are at the resolution of ERA-Interim (Dee et al., 2011) but produced with an updated model cycle nearly equivalent to that of ERA5 (while ERA-Interim used Cycle 31r2, implemented in 2006)—therefore, the difference between CAMSRA and ERA5 meteorology is likely almost entirely due to resolution, even more strictly than between ERA-Interim and ERA5. From each reanalysis, we obtained six-hourly zonal and meridional wind components, temperature, and specific humidity at model levels up to 50 hPa, and surface pressure.

BARTUSEK ET AL. 2 of 11

From CAMSRA, we also obtained ozone and a stratospheric ozone tracer (O₃S) at model levels up to 50 hPa and pressure levels 250, 500, and 850 hPa (interpolated from model levels for O₃S). Unlike other reanalyses that also assimilate ozone observations (such as NASA's MERRA-2 [Modern-Era Retrospective analysis for Research and Applications, version 2; Gelaro et al., 2017] and ERA5), CAMSRA employs a chemical transport model (CTM)—the Carbon Bond 2005 (CB05) chemistry mechanism (Flemming et al., 2015; Huijnen et al., 2010) integrated within IFS. While two previous ECMWF chemistry reanalyses (MACC and GEMS) also employed a CTM, it remained two-way coupled to IFS instead of directly integrated (on-line) within it, and while one other reanalysis employs a CTM (Tropospheric Chemical Reanalysis 2 [TCR-2] from NASA's Jet Propulsion Laboratory; Miyazaki et al., 2019) it is of much coarser resolution. Recent NASA coupled chemistry-meteorology products are likewise promising for studying stratospheric intrusions (MERRA2-GMI [Global Modeling Initiative] and GEOS-CF [Goddard Earth Observing System Composition Forecasts]; Strode et al., 2015; Keller et al., 2021; Knowland et al., 2022). CAMSRA ozone is broadly consistent with upper-tropospheric observations during stratospheric intrusions over Europe, despite overestimation in some sites (Akritidis et al., 2022), and lower-tropospheric ozone in East Asia (Park et al., 2020). Stratospheric ozone in CAMSRA is parameterized using the Cariolle scheme (Cariolle & Déqué, 1986; Cariolle & Teyssèdre, 2007), and subject to data assimilation. O₃S is identical to ozone (but without data assimilation) in the stratosphere, but once across the tropopause (a spatially-varying time-fixed pressure threshold) it is freely transported and subject to chemical loss and deposition, but not production. It therefore roughly represents the portion of tropospheric ozone deriving from the stratosphere, likely tending toward an upper limit.

To identify tropopause folding in CAMSRA and ERA5, we apply a modified version of the algorithm of Skerlak et al. (2015) (building on Sprenger et al., 2003; Skerlak et al., 2014). The algorithm first defines the dynamical tropopause as the lower of the ±2 Potential Vorticity Unit (PVU) or 380 K potential temperature surface. At each timestep, folding is identified in each atmospheric column in which the tropopause is crossed in the vertical three or more times. Pressure values of the three crossings (interpolated between model levels based on the PV profile) are saved: pmin and pmax are the pressures of the upper and lower crossings and dp is the pressure difference between the upper and middle crossings (Figure 1a). Folded columns are classified into three depth ranges: Shallow (50 hPa $\leq dp < 200$ hPa), Medium (200 hPa $\leq dp < 350$ hPa), and Deep ($dp \geq 350$ hPa), ignoring folding <50 hPa. However, high-PV anomalies can arise in the troposphere independently from folding (e.g., cut-off from the stratosphere, or generated by diabatic or surface frictional processes). Therefore, to avoid spuriously identifying folding, the algorithm labels each 3D grid cell as either troposphere, stratosphere, troposphere but high-PV, or stratosphere but low-PV. In our analysis, ERA5's high resolution necessitated modifications to the algorithm to avoid occasional classifications of the entire stratosphere as high-PV surface-connected (therefore tropospheric) air (see details in Supplementary Information). Comparing folding identification with versus without our modifications (in CAMSRA) shows them to be generally conservative, reducing folding frequency (Figure S1 in Supporting Information S1).

Analysis year 2012 was chosen in order to minimize discontinuities in assimilated ozone data and provide the most recent data free of known instrumentation biases affecting CAMSRA ozone from 2013 onwards (Inness et al., 2019; Wagner et al., 2021). Folding frequencies in 2012 are roughly consistent with the 1979–2014 average from ERA-Interim (Figure S1 in Supporting Information S1). Ozone and folding fields were deseasonalized by removing smoothed local monthly averages before correlation analysis.

3. Results

We first show an example of tropopause folding captured only at higher resolution: a latitudinal cross-section displays a fold in the ERA5 tropopause that CAMSRA's tropopause is too coarse to resolve (Figure 1a). Meanwhile, in this fold's vicinity, ozone (in CAMSRA) intrudes from the stratosphere into the troposphere—hence, while the ozone intrusion itself is resolved by CAMSRA, its relationship to folding is only captured by a higher-resolution tropopause (Knowland, Doherty, et al., 2017). More broadly, during the example time-step, folding is geographically much more widespread in ERA5, and reveals stronger correspondence with mid-tropospheric ozone, overlapping with many filamentary ozone structures that CAMSRA folding does not (Figures 1c and 1d). This improved correspondence generally persists across the 250, 500, and 850 hPa levels for both O₃ and stratosphere-sourced ozone (O₃S), although the folding—ozone relationship weakens in the tropics and at 850 hPa (Figure S2 in Supporting Information S1), emphasizing other production processes. This

BARTUSEK ET AL. 3 of 11

19448007, 2023, 8, Downloaded from https://agupubs.onlinelibrary.wiley.com/doi/10.1029/2022GL101690 by Columbia University Libraries, Wiley Online Library on [08/05/2023]. See the Terms and Conditions (https://onlinelibrary.wiley.

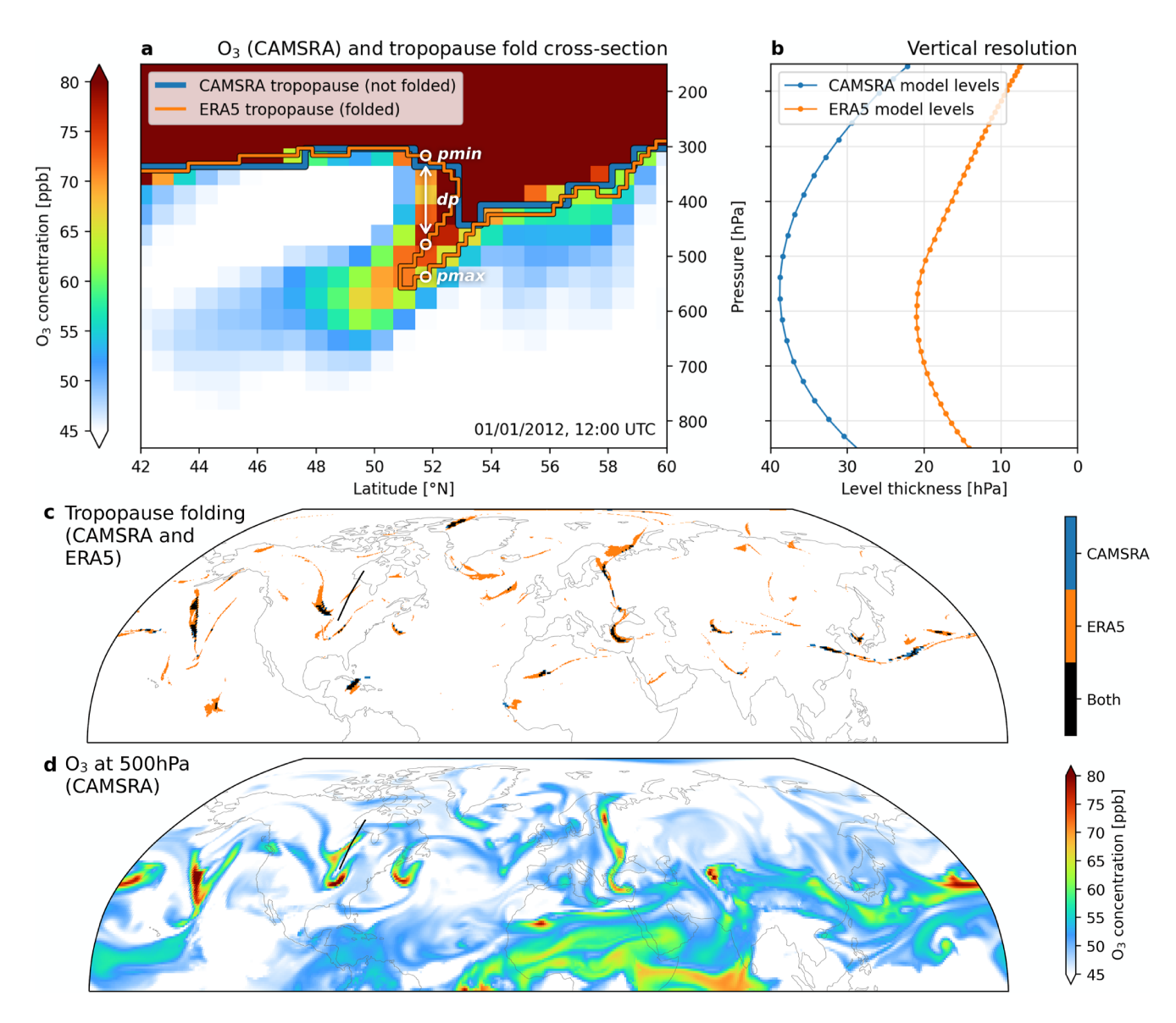


Figure 1. Comparison of tropopause folding, vertical resolution, and mid-tropospheric ozone in CAMSRA and ERA5. (a) Dynamical tropopauses in CAMSRA and ERA5, and ozone from CAMSRA, along a latitudinal cross-section (line in (c, d)) on 1 January 2012. ERA5's tropopause is folded throughout a range of columns (~ 51°–53°N); pressure parameters *pmin*, *dp*, and *pmax* produced by the folding identification algorithm (see Data and Methods) are illustrated for one column. Pressure is plotted using a 1013.25 hPa reference surface pressure. (b) Vertical resolution of CAMSRA and ERA5 model levels (pressure difference between interfaces) on the y-axis of (a); dots indicate level midpoints. (c, d) All columns with folding identified in CAMSRA, ERA5, or both (c), and 500 hPa ozone (d), during the example timestep.

cross-section suggests an important role for vertical resolution—ERA5's is at least roughly double CAMSRA's throughout the troposphere (Figure 1b)—while a geographic perspective also emphasizes horizontal resolution (Figures 1c and 1d). Overall, it appears common that ozone intrusions are only revealed to be associated with folding when the tropopause is seen at high-enough resolution.

Expanding our analysis to 1 year, we find that folding frequency increases nearly everywhere from CAMSRA to ERA5 (Figures 2a–2c). The frequency difference (Figure 2c) resembles the underlying distributions (largest along the subtropical jets [STJs], especially over the South Indian Ocean, Middle East, and North Africa), while most closely mirroring ERA5's. However, relative frequency differences (Figure 2d) reveal where CAMSRA particularly under-represents folding, highlighting areas with generally rarer folding. Over much of the extratropics, folding increases >10-fold between datasets; many areas with zero CAMSRA folding approach 2% in ERA5. Additionally, while absolute frequency increases are strongest for shallower folds, relative increases are strongest

BARTUSEK ET AL. 4 of 11

19448007, 2023, 8, Downloaded from https://agupubs.onlinclibrary.wiley.com/doi/10.1029/2022GL101690 by Columbia University Libraries, Wiley Online Library on [08/05/2023]. See the Terms

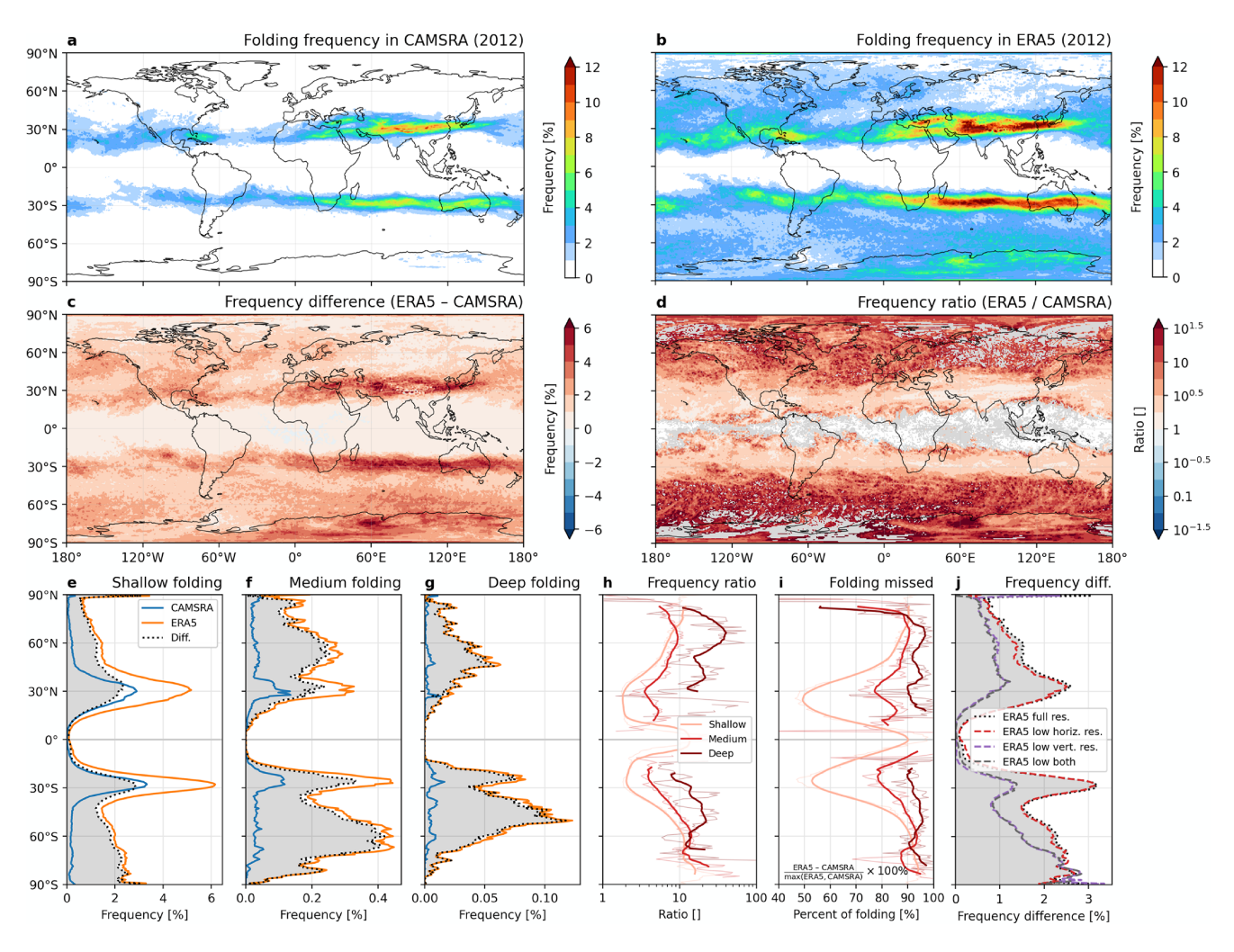


Figure 2. One-year tropopause folding frequencies in CAMSRA and ERA5. (a, b) Folding frequency throughout 2012, in percent of timesteps (ERA5 frequencies subsampled to CAMSRA's grid). (c, d) Frequency difference (ERA5–CAMSRA) and ratio (ERA5/CAMSRA). (e–g) Zonal-mean frequency of Shallow, Medium, and Deep folding (note *x*-axis scales). (h–i) Zonal-mean frequency ratio and percentage of folding missed by the lower-frequency data set in each gridcell (see formula) separated by depth range, with running 15° means. (j) Frequency difference (for all folding depths), comparing folding in ERA5 at various resolution configurations minus that in CAMSRA.

for deeper folds (Figures 2e–2i). In fact, zonal-mean distributions of Medium and Deep folding in CAMSRA (Figures 2f–2g) fail to capture to first order their prominent midlatitude peaks evident in ERA5. Zonal-mean frequency ratio (Figure 2h) and percentage of ERA5 folding missed by CAMSRA (Figure 2i) confirm that deeper folding is more likely to be uncaptured at low resolution. Specifically, while around half of ERA5 folding is missed by CAMSRA at its dominant latitudes (but nearly 90% on average), nearly 100% of Deep folding is missed almost everywhere (Figure 2i; Figure S3 in Supporting Information S1).

Importantly, coarsening ERA5 to CAMSRA's resolution in both dimensions and each alone (before calculating PV) reveals that folding frequency increases are almost entirely attributable to vertical resolution improvement (Figure 2j; Figure S4 in Supporting Information S1)—although ERA5 coarsened in both dimensions still identifies more folding than CAMSRA, implying some remaining effects of the initial model resolution, possibly including horizontal effects. Moreover, while folds are often thinner than the vertical resolution in CAMSRA, they largely occur at resolved scales in ERA5 (Figure S5 in Supporting Information S1), suggesting that such vertical resolutions may be necessary to fully resolve folding—<20 hPa (Figure 1b) or roughly 0.3 km throughout the troposphere (Hoffmann et al., 2019). Therefore, lower-resolution data disproportionately misses deeper folding likely because as intrusions extend deeper into the troposphere they tend to become more filamentary, hence more difficult to resolve vertically. Accordingly, maps of average depth of folding *dp* (Figure S6 in Supporting

BARTUSEK ET AL. 5 of 11

19448007, 2023, 8, Downloaded from https://agupubs.onlinelibrary.wiley.com/doi/10.1029/2022GL101690 by Columbia University Libraries, Wiley Online Library on [08/05/2023]. See the

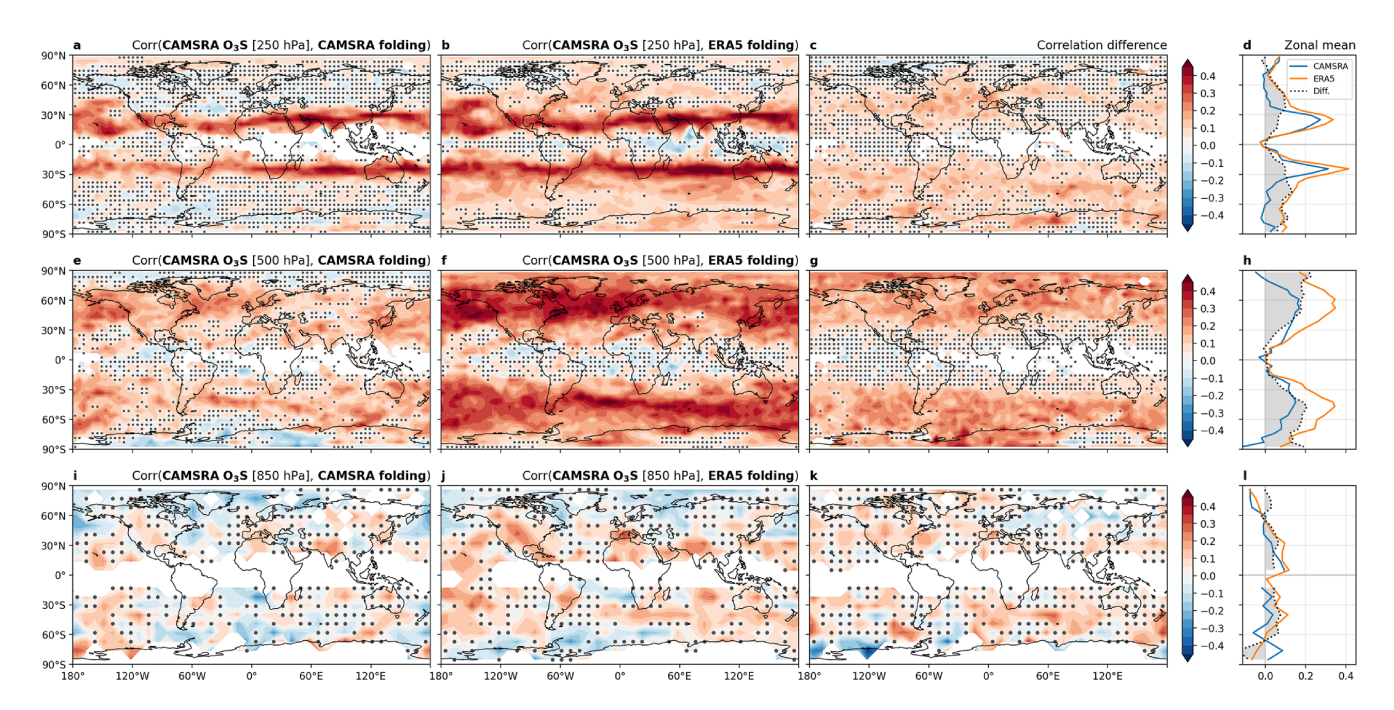


Figure 3. Correlations between tropopause folding and CAMSRA ozone at three pressure levels. (a) Spearman's rank correlation between folding occurrence in CAMSRA and stratospheric ozone tracer (O_3 S, from CAMSRA) at 250 hPa, throughout 2012, dotted where insignificant (at the 0.05 level). (b) As in (a) but for ERA5 folding. In other words, between (a) and (b) the same O_3 S field is correlated against two different folding fields. (c) Difference in correlation coefficients, dotted where insignificant. (d) Zonal means of (a–c). (e–l) As in (a–d) but for O_3 S at 500 and 850 hPa. Before correlating, fields are coarsened to $4.5^{\circ} \times 4.5^{\circ}$ (250, 500 hPa) or $9^{\circ} \times 9^{\circ}$ (850 hPa), and smoothed by 1-day (500 hPa) or 3-day (850 hPa) running means, to better capture non-local ozone impacts of folding; only Medium and Deep folding is considered at 850 hPa.

Information S1) strongly predict that of frequency ratio (Figure 2d). This underestimation of specifically deeper intrusions may be consequential toward capturing folding's relationship with tropospheric ozone: therefore, we next investigate the influence of folding resolution on temporal correlations between folding activity and ozone STT.

Accompanying more frequent folding with increased resolution, the correlation between folding and tropospheric O_3S (to most directly reflect STT) significantly strengthens, outside the tropics (Figure 3). The relationship between folding and 250 hPa O₃S closely follows underlying fold frequency distributions (Figures 2a, 2b, and 2e): correlation maximizes along STJs, reaching 0.40 for CAMSRA and 0.45 for ERA5, and generally strengthens with higher folding frequency (Figures 3a-3d). However, correlations strengthen most where relative (Figure 2d) rather than absolute (Figure 2c) frequency differences are highest, increasing by ~0.2 from near-zero in CAMSRA throughout much of the extratropics (where 250 hPa most represents the upper-troposphere-lower-stratosphere region). At 500 hPa, O₃S is most correlated to folding in the extratropics, emphasizing storm tracks rather than STJs (Figures 3e, 3f, and 3h). Correlations strongly mirror folding depth (Figure S6 in Supporting Information S1), implying that deeper midlatitude folds, though rarer than STJ-related folds, are more powerfully associated with mid-tropospheric ozone. O₃S at 500 hPa is roughly twice as correlated (or roughly four times as attributable) to ERA5 folding as to CAMSRA folding, reaching ~0.4 over widespread regions, and correlation increases again reflect distributions of relative frequency increases and Medium and Deep folding differences (Figure S7 in Supporting Information S1). At 850 hPa, O₃S is much less correlated with folding overall (Figures 3i, 3j, and 3l), perhaps partially reflecting that folding-related ozone impacts may be spatially offset from folding itself after transport into the lower troposphere. However, O₃S correlation with ERA5 folding reveals maxima in known hotspots of strong stratospheric and folding influence on near-surface ozone (not well captured by CAMSRA folding), including western North America, the Tibetan Plateau, the Mediterranean, and storm track regions (Skerlak et al., 2014). Correlation differences most closely follow Deep fold frequency increases—strongest over midlatitude storm tracks and North America (Figure 3k).

Since O_3S 's stronger relation to ERA5 than CAMSRA folding occurs with more frequent folding, we argue that ozone STT may be more attributable to folding than low-resolution folding implies. In other words, ozone STT occurring without folding in CAMSRA is revealed to occur in the vicinity of folding at smaller scales, as

BARTUSEK ET AL. 6 of 11

19448007, 2023, 8, Downloaded from https://agupubs.onlinclibrary.wiley.com/doi/10.1029/2022GL101690 by Columbia University Libraries, Wiley Online Library on [08/05/2023]. See the Terms

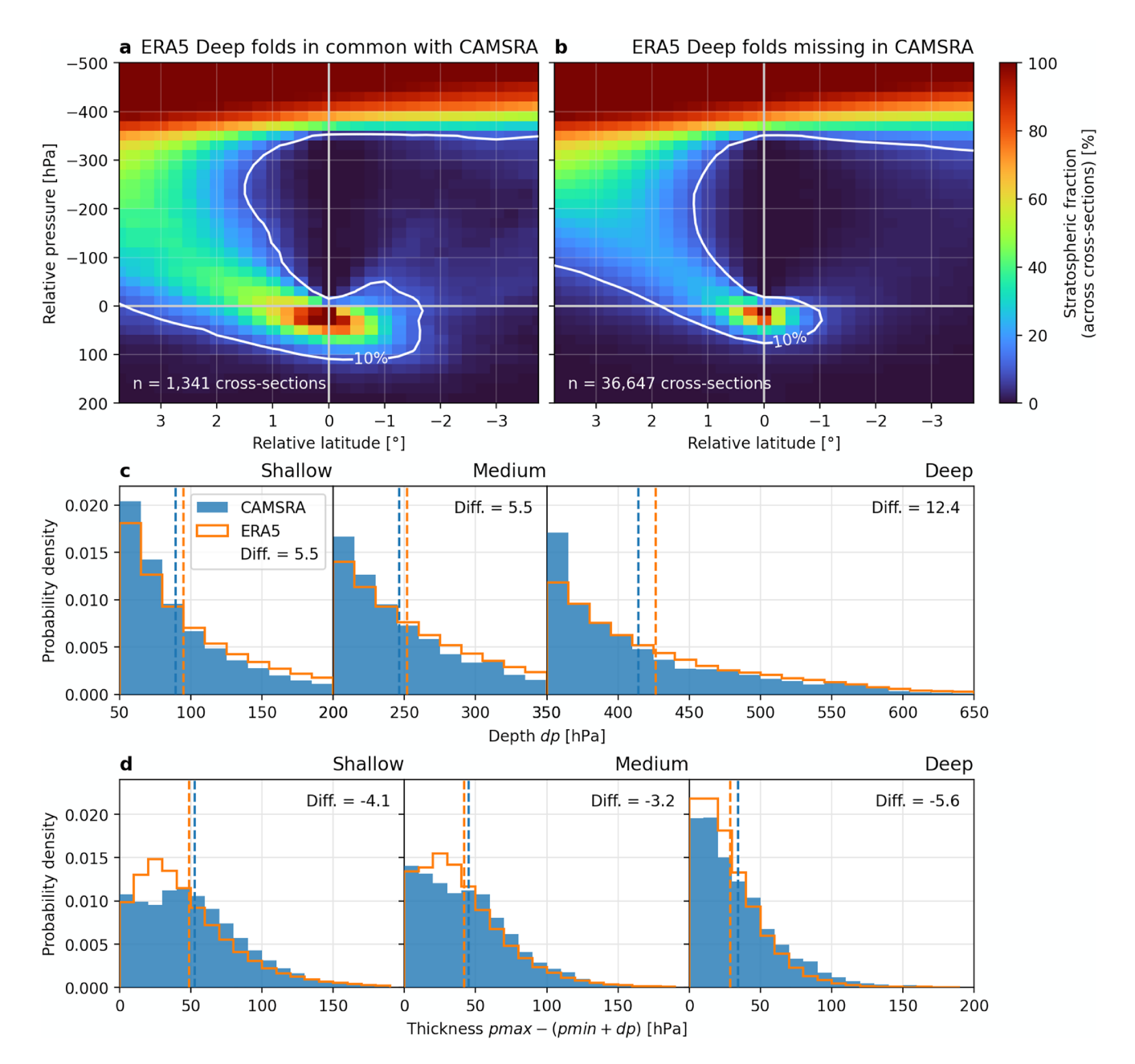


Figure 4. Tropopause folding morphology in CAMSRA and ERA5. (a, b) Composited latitudinal cross-sections of Deep folds in ERA5 (i.e., throughout ranges of columns where folding depth dp exceeds 350 hPa, centered horizontally on the column of smallest dp and vertically on that column's middle tropopause crossing), for folding identified in both ERA5 and CAMSRA simultaneously (a) versus only in ERA5 (b). The composited field is a binary label delineating troposphere versus stratosphere, producing an average fold morphology; the 10% stratospheric contour is indicated. (c) Histograms of dp for folding in CAMSRA and ERA5 in each depth category, with means compared. (d) As in (c) but for folding thickness (the pressure difference between the lowest and middle tropopause crossings, pmax - (pmin + dp)).

suggested by Figure 1. Altogether, correlations strengthen most at the approximate latitudes of maximum ozone STT—in midlatitudes, poleward of STJs (Hsu & Prather, 2009; Skerlak et al., 2014)—implying the relevance of these changes for overall STT. Furthermore, Figure 3's correlation results are generally consistent when substituting ozone for O₃S (Figure S8 in Supporting Information S1)—except at 850 hPa, where its drivers are very diverse—suggesting that folding-related O₃S is important to free-tropospheric ozone overall.

Following Figure 3's indication of deeper folding's role in strengthening ozone correlations, we directly investigate fold morphology, confirming that higher-resolution folding is both deeper and thinner, especially for Deep folding (Figure 4). We compare composited cross-sections of Deep folds in ERA5 captured by both CAMSRA and ERA5

BARTUSEK ET AL. 7 of 11

with those only captured by ERA5 (Figures 4a and 4b). To compare fold morphology, we composite a binary label field that geometrically delineates the stratosphere and troposphere. Cross-sections are fixed around folds' column of minimum depth and their middle tropopause crossing in that column, so that fold depth (negative pressures) and thickness (positive pressures) can be simultaneously visualized. These cross-sections capture only folds' latitudinal component; however, we note that even primarily-longitudinal folds likely still express in latitude (e.g., Figure 1). Qualitatively, folds only captured by ERA5 are thinner, with their 10% stratospheric contour extending less far below their middle tropopause surface—however, depth differences are less clear (Figures 4a and 4b). Histograms of depth and thickness (Figures 4c and 4d) reveal more quantitatively that with increasing resolution, folding becomes deeper but thinner, consistently across folding depth categories (geospatially resolved in Figure S9 in Supporting Information S1). Deep folding is most affected, becoming on average 12 hPa deeper and 6 hPa thinner. Furthermore, in columns where ERA5 identifies Deep folding but CAMSRA fails, CAMSRA almost exclusively identifies no folding rather than simulating Medium or Shallow folding (Figure S10 in Supporting Information S1), confirming that CAMSRA specifically underresolves the tips of intrusions rather than simulating the wrong depth.

Figure 4 therefore provides evidence that resolving deeper, thinner folding is particularly responsible for uncovering stronger relationships between folding and tropospheric ozone. Specifically, with higher-resolution folding, ozone anomalies at greater distance from the dynamical tropopause remain attributable to folding activity, as epitomized by Figure 1a: the fold tip in ERA5 extends deeper than in CAMSRA (which finds no fold), overlapping with more of the underlying ozone intrusion and thereby revealing that deeper parts of it are attributable to folding. As Figures 1 and 3 show, in such cases, the transport itself occurs at scales larger than the ERA5-identified folding: CAMSRA ozone is advected by resolved winds, entering the troposphere despite an unfolded (coarsely-resolved) tropopause. This suggests that alternative features besides folding may correspond well with ozone STT: indeed, O3S is well-correlated with dryness (nearly everywhere) and descent (mostly in the lower troposphere) in CAMSRA, providing potential low-resolution proxies for ozone STT that can surpass CAMSRA folding and compare with ERA5 folding (Figure S11 in Supporting Information S1).

4. Conclusions and Discussion

In this study, we identified tropopause folding in two reanalyses—high-resolution ERA5 and lower-resolution chemical reanalysis CAMSRA (providing nearly identical meteorology but at the resolution of ERA-Interim). We compared the distribution and characteristics of folding in ERA5 (the highest-resolution reanalysis investigation of folding to date) to those in CAMSRA, and assessed the relationships of both folding datasets with ozone from CAMSRA, to examine folding's role in the behavior of tropospheric ozone and its transport from the stratosphere. Our findings corresponding to the research questions in the Introduction are as follows:

- 1. Higher-resolution folding is markedly more frequent. Between datasets, frequency increases most along the subtropical jets and for shallower folds, but increases *relatively* most in the extratropics and for deeper folds (roughly 10–100-times). Deep folding is nearly entirely unrepresented at lower resolution, versus about half of shallow folding at its dominant latitudes. Increased folding derives nearly entirely from vertical resolution (which roughly doubles), even though horizontal resolution increases more (9-fold).
- 2. Higher-resolution folding reveals significantly stronger correlations between folding and upper- and mid-tropospheric O₃S (stratospheric ozone tracer), especially where relative fold frequency increases are greatest and folds are deeper. Higher-resolution folding's correlation with near-surface O₃S highlights known hotspots of stratospheric ozone influence uncaptured by low-resolution folding. Correlations of folding with O₃S and with ozone are largely consistent with each other (above 850 hPa).
- 3. Increased resolution reveals folding to be deeper and thinner, suggesting that such folding may contribute significantly to folding—ozone correlations.
- 4. Our results suggest that ozone STT and tropospheric ozone are more systematically associated with tropopause folding than implied based on low-resolution folding. Specifically, in places where ozone STT occurs despite an unfolded (coarsely-resolved) tropopause in CAMSRA, much is revealed to be associated with smaller-scale folding only visible at higher resolution. Meanwhile, we show that dryness and descent could potentially provide low-resolution proxies of ozone STT comparable to high-resolution folding.

Research has long indicated the significance of folding to STT: localized observational and process-based studies have demonstrated strong ozone STT within intrusions extending deep into the troposphere, while broader-scale studies have shown folding's role in STT of air and noted the important influence of stratospheric ozone variability on tropospheric ozone (Hess et al., 2015; Langford et al., 1996, 2009; Langford & Reid, 1998; Lefohn

BARTUSEK ET AL. 8 of 11

et al., 2012; Neu et al., 2014; Ott et al., 2016; Skerlak et al., 2019; Stohl et al., 2003; Wang et al., 2020; Williams et al., 2019). However, an investigation of folding's relationship with ozone STT that is systematic and global while based on data with high chemical and meteorological fidelity is lacking, despite recent developments in coupled chemistry and meteorology products (including those not analyzed here, e.g., MERRA2-GMI and GEOS-CF). Here, we provide systematic evidence that higher-resolution folding accounts for a larger proportion of ozone STT than lower-resolution folding. Our findings are specifically consistent with midlatitude-cyclone-associated folding representing a primary STT mechanism (Jaeglé et al., 2017; Knowland, Doherty, et al., 2017). We show that, although ozone STT is known to be strongest along storm tracks (Hsu & Prather, 2009; Skerlak et al., 2014), its linkage with folding in these areas has remained uncaptured by low-resolution folding climatologies, which underrepresent midlatitude folding due to its smaller scales.

Furthermore, the particular importance of thinner and deeper folding to tropospheric ozone underscores that transport in the stable, highly-sheared free troposphere dominantly occurs in thin layers and plumes that filament, resisting diffusion (Heald et al., 2003; Newell et al., 1999; Stoller et al., 1999; Thouret et al., 2000). These high-concentration layers can enable strong localized stratospheric influence on near-surface (Trickl et al., 2010, 2020) and mid-tropospheric (Trickl et al., 2011) ozone. However, current global models fail to represent transport plumes' observed persistence due to (dominantly vertical) resolution-related diffusion (Eastham & Jacob, 2017; Zhuang et al., 2018). Our results suggest that vertical resolution similar to ERA5 (<20 hPa or roughly 0.3 km throughout the free troposphere) may be necessary to resolve tropopause folding, and emphasize its importance over horizontal resolution for representing such filamentary dynamical and transport processes in reanalysis and model simulations.

Data Availability Statement

All reanalysis data is publicly available from the ECMWF at https://doi.org/10.24381/cds.bd0915c6 (ERA5) and https://ads.atmosphere.copernicus.eu/cdsapp#!/dataset/cams-global-reanalysis-eac4?tab=overview (CAMSRA). The tropopause folding identification algorithm and code to reproduce the main and supplementary figures is available at http://doi.org/10.5281/zenodo.7764851.

References

Akritidis, D., Pozzer, A., Flemming, J., Inness, A., Nédélec, P., & Zanis, P. (2022). A process-oriented evaluation of cams reanalysis ozone during tropopause folds over Europe for the period 2003-2018. Atmospheric Chemistry and Physics Discussions, 22(9), 1-23. https://doi. org/10.5194/acp-22-6275-2022

Akritidis, D., Pozzer, A., Flemming, J., Inness, A., & Zanis, P. (2021). A global climatology of tropopause folds in CAMS and MERRA-2 reanalyses. Journal of Geophysical Research: Atmospheres, 126(8), e2020JD034115. https://doi.org/10.1029/2020JD034115

Akritidis, D., Pozzer, A., & Zanis, P. (2019). On the impact of future climate change on tropopause folds and tropospheric ozone. Atmospheric Chemistry and Physics, 19(22), 14387–14401. https://doi.org/10.5194/acp-19-14387-2019

Akritidis, D., Pozzer, A., Zanis, P., Tyrlis, E., Škerlak, B., Sprenger, M., & Lelieveld, J. (2016). On the role of tropopause folds in summertime tropospheric ozone over the eastern Mediterranean and the Middle East. Atmospheric Chemistry and Physics, 16(21), 14025–14039. https:// doi.org/10.5194/acp-16-14025-2016

Appenzeller, C., & Davies, H. C. (1992). Structure of stratospheric intrusions into the troposphere. Nature, 358(6387), 570-572. https://doi. org/10.1038/358570a0

Appenzeller, C., Davies, H. C., & Norton, W. A. (1996). Fragmentation of stratospheric intrusions. Journal of Geophysical Research, 101(D1), 1435-1456. https://doi.org/10.1029/95JD02674

Banerjee, A., Maycock, A. C., Archibald, A. T., Abraham, N. L., Telford, P., Braesicke, P., & Pyle, J. A. (2016). Drivers of changes in stratospheric and tropospheric ozone between year 2000 and 2100. Atmospheric Chemistry and Physics, 16(5), 2727-2746. https://doi.org/10.5194/ acp-16-2727-2016

Beekmann, M., Ancellet, G., Blonsky, S., De Muer, D., Ebel, A., Elbern, H., et al. (1997). Regional and global tropopause fold occurrence and related ozone flux across the tropopause. Journal of Atmospheric Chemistry, 28(1), 29-44. https://doi.org/10.1023/A:1005897314623

Boothe, A. C., & Homeyer, C. R. (2017). Global large-scale stratosphere-troposphere exchange in modern reanalyses. Atmospheric Chemistry and Physics, 17(9), 5537-5559. https://doi.org/10.5194/acp-17-5537-2017

Buker, M. L., Hitchman, M. H., Tripoli, G. J., Pierce, R. B., Browell, E. V., & Avery, M. A. (2005). Resolution dependence of cross-tropopause ozone transport over East Asia. Journal of Geophysical Research, 110(D3), D03107. https://doi.org/10.1029/2004jd004739

Cariolle, D., & Déqué, M. (1986). Southern hemisphere medium-scale waves and total ozone disturbances in a spectral general circulation model. Journal of Geophysical Research, 91(D10), 10825-10846. https://doi.org/10.1029/JD091iD10p10825

Cariolle, D., & Teyssèdre, H. (2007). A revised linear ozone photochemistry parameterization for use in transport and general circulation models: Multi-annual simulations, Atmospheric Chemistry and Physics, 7(9), 2183-2196. https://doi.org/10.5194/acp-7-2183-2007

Chen, X., Añel, J. A., Su, Z., de la Torre, L., van Kelder, H., Peet, J. v., & Ma, Y. (2013). The deep atmospheric boundary layer and its significance to the stratosphere and troposphere exchange over the Tibetan plateau. PLoS One, 8(2), e56909. https://doi.org/10.1371/journal.pone.0056909 Chen, X. L., Ma, Y. M., Kelder, H., Su, Z., & Yang, K. (2011). On the behaviour of the tropopause folding events over the Tibetan plateau. Atmospheric Chemistry and Physics, 11(10), 5113-5122. https://doi.org/10.5194/acp-11-5113-2011

Danielsen, E. F. (1959). The laminar structure of the atmosphere and its relation to the concept of a tropopause. Archiv für Meteorologie, Geophysik und Bioklimatologie, Serie A, 11(3), 293-332. https://doi.org/10.1007/BF02247210

Acknowledgments

This work was supported by NSF Award AGS-1802248 (S. B. and Y. W.) and NSF OPP-1825858 (M. T., Y. W. and C. Z.). We thank K. Emma Knowland and two anonymous peer reviewers for their valuable contributions that greatly improved the quality of the manuscript.

BARTUSEK ET AL. 9 of 11

- Danielsen, E. F. (1968). Stratospheric-tropospheric exchange based on radioactivity, ozone and potential vorticity. *Journal of the Atmospheric Sciences*, 25(3), 502–518. https://doi.org/10.1175/1520-0469(1968)025\000f30502:STEBOR\000f32.0.CO;2
- Dee, D. P., Uppala, S. M., Simmons, A. J., Berrisford, P., Poli, P., Kobayashi, S., et al. (2011). The ERA-Interim reanalysis: Configuration and performance of the data assimilation system. *Quarterly Journal of the Royal Meteorological Society*, 137(656), 553–597. https://doi.org/10.1002/qj.828
- Dragani, R. (2010). On the quality of the ERA-interim ozone reanalyses. Part II comparisons with satellite data. ECMWF.
- Eastham, S. D., & Jacob, D. J. (2017). Limits on the ability of global Eulerian models to resolve intercontinental transport of chemical plumes. Atmospheric Chemistry and Physics, 17(4), 2543–2553. https://doi.org/10.5194/acp-17-2543-2017
- Flemming, J., Huijnen, V., Arteta, J., Bechtold, P., Beljaars, A., Blechschmidt, A.-M., et al. (2015). Tropospheric chemistry in the integrated forecasting system of ecmwf. *Geoscientific Model Development*, 8(4), 975–1003. https://doi.org/10.5194/gmd-8-975-2015
- Fu, T.-M., & Tian, H. (2019). Climate change penalty to ozone air quality: Review of current understandings and knowledge gaps. Current Pollution Reports, 5(3), 159–171. https://doi.org/10.1007/s40726-019-00115-6
- Gelaro, R., McCarty, W., Suárez, M. J., Todling, R., Molod, A., Takacs, L., et al. (2017). The modern-era retrospective analysis for research and applications, version 2 (MERRA-2). *Journal of Climate*, 30(14), 5419–5454. https://doi.org/10.1175/jcli-d-16-0758.1
- Heald, C. L., Jacob, D. J., Fiore, A. M., Emmons, L. K., Gille, J. C., Deeter, M. N., et al. (2003). Asian outflow and trans-pacific transport of carbon monoxide and ozone pollution: An integrated satellite, aircraft, and model perspective. *Journal of Geophysical Research*, 108(D24). https://doi.org/10.1029/2003jd003507
- Hegglin, M. I., & Shepherd, T. G. (2009). Large climate-induced changes in ultraviolet index and stratosphere-to-troposphere ozone flux. *Nature Geoscience*, 2(10), 687–691. https://doi.org/10.1038/ngeo604
- Hersbach, H., Bell, B., Berrisford, P., Hirahara, S., Horányi, A., Muñoz-Sabater, J., et al. (2020). The ERA5 global reanalysis. *Quarterly Journal of the Royal Meteorological Society*, 146(730), 1999–2049. https://doi.org/10.1002/qj.3803
- Hess, P., Kinnison, D., & Tang, Q. (2015). Ensemble simulations of the role of the stratosphere in the attribution of northern extratropical tropospheric ozone variability. *Atmospheric Chemistry and Physics*, 15(5), 2341–2365. https://doi.org/10.5194/acp-15-2341-2015
- Hoffmann, L., Günther, G., Li, D., Stein, O., Wu, X., Griessbach, S., et al. (2019). From ERA-Interim to ERA5: The considerable impact of ECMWF's next-generation reanalysis on Lagrangian transport simulations. *Atmospheric Chemistry and Physics*, 19(5), 3097–3124. https://doi.org/10.5194/acp-19-3097-2019
- Hoffmann, L., & Spang, R. (2022). An assessment of tropopause characteristics of the ERA5 and ERA-Interim meteorological reanalyses. *Atmospheric Chemistry and Physics*, 22(6), 4019–4046. https://doi.org/10.5194/acp-22-4019-2022
- Hsu, J., & Prather, M. J. (2009). Stratospheric variability and tropospheric ozone. *Journal of Geophysical Research*, 114(D6), D06102. https://doi.org/10.1029/2008id010942
- Huijnen, V., Williams, J., van Weele, M., van Noije, T., Krol, M., Dentener, F., et al. (2010). The global chemistry transport model TM5: Description and evaluation of the tropospheric chemistry version 3.0. *Geoscientific Model Development*, 3(2), 445–473. https://doi.org/10.5194/gmd-3-445-2010
- Inness, A., Ades, M., Agustí-Panareda, A., Barré, J., Benedictow, A., Blechschmidt, A.-M., et al. (2019). The CAMS reanalysis of atmospheric composition. Atmospheric Chemistry and Physics, 19(6), 3515–3556. https://doi.org/10.5194/acp-19-3515-2019
- Jaeglé, L., Wood, R., & Wargan, K. (2017). Multiyear composite view of ozone enhancements and stratosphere-to-troposphere transport in dry intrusions of northern hemisphere extratropical cyclones. *Journal of Geophysical Research: Atmospheres*, 122(24), 13436–13457. https://doi.org/10.1002/2017JD027656
- Keller, C. A., Knowland, K. E., Duncan, B. N., Liu, J., Anderson, D. C., Das, S., et al. (2021). Description of the NASA GEOS composition forecast modeling system GEOS-CF v1.0. *Journal of Advances in Modeling Earth Systems*, 13(4), e2020MS002413. https://doi.org/10.1029/2020ms002413
- Knowland, K. E., Doherty, R. M., Hodges, K. I., & Ott, L. E. (2017). The influence of mid-latitude cyclones on European background surface ozone. Atmospheric Chemistry and Physics, 17(20), 12421–12447. https://doi.org/10.5194/acp-17-12421-2017
- Knowland, K. E., Keller, C. A., Wales, P. A., Wargan, K., Coy, L., Johnson, M. S., et al. (2022). NASA GEOS composition forecast modeling system GEOS-CF v1.0: Stratospheric composition. *Journal of Advances in Modeling Earth Systems*, 14(6). https://doi.org/10.1029/2021ms002852
- Knowland, K. E., Ott, L. E., Duncan, B. N., & Wargan, K. (2017). Stratospheric intrusion-influenced ozone air quality exceedances investigated in the NASA MERRA-2 reanalysis. Geophysical Research Letters, 44(20), 10691–10701. https://doi.org/10.1002/2017GL074532
- Krzyzanowski, M., & Cohen, A. (2008). Update of who air quality guidelines. Air Quality, Atmosphere & Health, 1(1), 7–13. https://doi.org/10.1007/s11869-008-0008-9
- Langford, A., Aikin, K., Eubank, C., & Williams, E. (2009). Stratospheric contribution to high surface ozone in Colorado during springtime. Geophysical Research Letters, 36(12), L12801. https://doi.org/10.1029/2009gl038367
- Langford, A., Masters, C., Proffitt, M., Hsie, E.-Y., & Tuck, A. (1996). Ozone measurements in a tropopause fold associated with a cut-off low system. Geophysical Research Letters, 23(18), 2501–2504. https://doi.org/10.1029/96gl02227
- Langford, A., & Reid, S. (1998). Dissipation and mixing of a small-scale stratospheric intrusion in the upper troposphere. *Journal of Geophysical Research*, 103(D23), 31265–31276. https://doi.org/10.1029/98jd02596
- Lefohn, A. S., Wernli, H., Shadwick, D., Oltmans, S. J., & Shapiro, M. (2012). Quantifying the importance of stratospheric-tropospheric transport on surface ozone concentrations at high- and low-elevation monitoring sites in the United States. *Atmospheric Environment*, 62, 646–656. https://doi.org/10.1016/j.atmosenv.2012.09.004
- Lin, M., Fiore, A. M., Cooper, O. R., Horowitz, L. W., Langford, A. O., Levy, H., et al. (2012). Springtime high surface ozone events over the western United States: Quantifying the role of stratospheric intrusions. *Journal of Geophysical Research*, 117(D21). https://doi.org/10.1029/2012jd018151
- Lin, M., Fiore, A. M., Horowitz, L. W., Langford, A. O., Oltmans, S. J., Tarasick, D., & Rieder, H. E. (2015). Climate variability modulates western US ozone air quality in spring via deep stratospheric intrusions. *Nature Communications*, 6(11), 7105. https://doi.org/10.1038/ncomms8105
- Meul, S., Langematz, U., Kröger, P., Oberländer-Hayn, S., & Jöckel, P. (2018). Future changes in the stratosphere-to-troposphere ozone mass flux and the contribution from climate change and ozone recovery. *Atmospheric Chemistry and Physics*, 18(10), 7721–7738. https://doi.org/10.5194/acp-18-7721-2018
- Miyazaki, K., Sekiya, T., Fu, D., Bowman, K., Kulawik, S., Sudo, K., et al. (2019). Balance of emission and dynamical controls on ozone during the Korea-United States air quality campaign from multiconstituent satellite data assimilation. *Journal of Geophysical Research: Atmospheres*, 124(1), 387–413. https://doi.org/10.1029/2018jd028912
- Monks, P. S., Archibald, A. T., Colette, A., Cooper, O., Coyle, M., Derwent, R., et al. (2015). Tropospheric ozone and its precursors from the urban to the global scale from air quality to short-lived climate forcer. *Atmospheric Chemistry and Physics*, 15(15), 8889–8973. https://doi.org/10.5194/acp-15-8889-2015

BARTUSEK ET AL. 10 of 11

- Myhre, G., Shindell, D., Bréon, F.-M., Collins, W., Fuglestvedt, J., Huang, J., et al. (2013). Anthropogenic and natural radiative forcing. In T. F. Stocker, D. Qin, G.-K. Plattner, M. Tignor, S. K. Allen, J. Boschung, et al. (Eds.), Climate change 2013: The physical science basis. contribution of working group i to the fifth assessment report of the intergovernmental panel on climate change (pp. 659–740). Cambridge University Press. https://doi.org/10.1017/CBO9781107415324.018
- Neu, J. L., Flury, T., Manney, G. L., Santee, M. L., Livesey, N. J., & Worden, J. (2014). Tropospheric ozone variations governed by changes in stratospheric circulation. *Nature Geoscience*, 7(5), 340–344. https://doi.org/10.1038/ngeo2138
- Newell, R. E., Thouret, V., Cho, J. Y. N., Stoller, P., Marenco, A., & Smit, H. G. (1999). Ubiquity of quasi-horizontal layers in the troposphere. Nature, 398(67256725), 316–319. https://doi.org/10.1038/18642
- Newell, R. E., Wu, Z.-X., Zhu, Y., Hu, W., Browell, E. V., Gregory, G. L., et al. (1996). Vertical fine-scale atmospheric structure measured from NASA DC-8 during PEM-West A. *Journal of Geophysical Research*, 101(D1), 1943–1960. https://doi.org/10.1029/95JD02613
- Ott, L. E., Duncan, B. N., Thompson, A. M., Diskin, G., Fasnacht, Z., Langford, A. O., et al. (2016). Frequency and impact of summertime stratospheric intrusions over Maryland during DISCOVER-AQ (2011): New evidence from NASA's GEOS-5 simulations. *Journal of Geophysical Research: Atmospheres*, 121(7), 3687–3706. https://doi.org/10.1002/2015jd024052
- Park, S., Son, S.-W., Jung, M.-I., Park, J., & Park, S. S. (2020). Evaluation of tropospheric ozone reanalyses with independent ozonesonde observations in East Asia. *Geoscience Letters*, 7(1), 12. https://doi.org/10.1186/s40562-020-00161-9
- Shapiro, M. A. (1980). Turbulent mixing within tropopause folds as a mechanism for the exchange of chemical constituents between the stratosphere and troposphere. *Journal of the Atmospheric Sciences*, 37(5), 994–1004. https://doi.org/10.1175/1520-0469(1980)037(0994:TMWTFA)2.0.CO;2
- Skerlak, B., Pfahl, S., Sprenger, M., & Wernli, H. (2019). A numerical process study on the rapid transport of stratospheric air down to the surface over western North America and the Tibetan plateau. Atmospheric Chemistry and Physics, 19(9), 6535–6549. https://doi.org/10.5194/acp-19-6535-2019
- Skerlak, B., Sprenger, M., Pfahl, S., Tyrlis, E., & Wernli, H. (2015). Tropopause folds in ERA-interim: Global climatology and relation to extreme weather events. *Journal of Geophysical Research: Atmospheres*, 120(10), 4860–4877. https://doi.org/10.1002/2014JD022787
- Skerlak, B., Sprenger, M., & Wernli, H. (2014). A global climatology of stratosphere–troposphere exchange using the ERA-interim data set from 1979 to 2011. Atmospheric Chemistry and Physics, 14(2), 913–937. https://doi.org/10.5194/acp-14-913-2014
- Spreitzer, E., Attinger, R., Boettcher, M., Forbes, R., Wernli, H., & Joos, H. (2019). Modification of potential vorticity near the tropopause by nonconservative processes in the ECMWF model. *Journal of the Atmospheric Sciences*, 76(6), 1709–1726. https://doi.org/10.1175/ias-d-18-0295.1
- Sprenger, M., Maspoli, M. C., & Wernli, H. (2003). Tropopause folds and cross-tropopause exchange: A global investigation based upon ECMWF analyses for the time period march 2000 to February 2001. *Journal of Geophysical Research*, 108(D12), 8518. https://doi.org/10.1029/2002JD002587
- Sprenger, M., & Wernli, H. (2003). A northern hemispheric climatology of cross-tropopause exchange for the ERA15 time period (1979–1993). Journal of Geophysical Research, 108(D12), 8521. https://doi.org/10.1029/2002jd002636
- Stohl, A., Bonasoni, P., Cristofanelli, P., Collins, W., Feichter, J., Frank, A., et al. (2003). Stratosphere-troposphere exchange: A review, and what we have learned from staccato. *Journal of Geophysical Research*, 108(D12), 8516. https://doi.org/10.1029/2002JD002490
- Stoller, P., Cho, J. Y. N., Newell, R. E., Thouret, V., Zhu, Y., Carroll, M. A., et al. (1999). Measurements of atmospheric layers from the NASA DC-8 and P-3B aircraft during PEM-Tropics A. *Journal of Geophysical Research*, 104(D5), 5745–5764. https://doi.org/10.1029/98JD02717
- Strode, S. A., Rodriguez, J. M., Logan, J. A., Cooper, O. R., Witte, J. C., Lamsal, L. N., et al. (2015). Trends and variability in surface ozone over the United States. *Journal of Geophysical Research: Atmospheres*, 120(17), 9020–9042. https://doi.org/10.1002/2014jd022784
- Thouret, V., Cho, J. Y. N., Newell, R. E., Marenco, A., & Smit, H. G. J. (2000). General characteristics of tropospheric trace constituent layers observed in the MOZAIC program. *Journal of Geophysical Research*, 105(D13), 17379–17392. https://doi.org/10.1029/2000JD900238
- Trickl, T., Bärtsch-Ritter, N., Eisele, H., Furger, M., Mücke, R., Sprenger, M., & Stohl, A. (2011). High-ozone layers in the middle and upper troposphere above central Europe: Potential import from the stratosphere along the subtropical jet stream. *Atmospheric Chemistry and Physics*, 11(17), 9343–9366. https://doi.org/10.5194/acp-11-9343-2011
- Trickl, T., Feldmann, H., Kanter, H.-J., Scheel, H.-E., Sprenger, M., Stohl, A., & Wernli, H. (2010). Forecasted deep stratospheric intrusions over central Europe: Case studies and climatologies. *Atmospheric Chemistry and Physics*, 10(2), 499–524. https://doi.org/10.5194/acp-10-499-2010
- Trickl, T., Vogelmann, H., Ries, L., & Sprenger, M. (2020). Very high stratospheric influence observed in the free troposphere over the northern Alps—Just a local phenomenon? *Atmospheric Chemistry and Physics*, 20(1), 243–266. https://doi.org/10.5194/acp-20-243-2020
- Tyrlis, E., Skerlak, B., Sprenger, M., Wernli, H., Zittis, G., & Lelieveld, J. (2014). On the linkage between the Asian summer monsoon and tropopause fold activity over the eastern Mediterranean and the Middle East. *Journal of Geophysical Research: Atmospheres*, 119(6), 3202–3221. https://doi.org/10.1002/2013JD021113
- Wagner, A., Bennouna, Y., Blechschmidt, A.-M., Brasseur, G., Chabrillat, S., Christophe, Y., et al. (2021). Comprehensive evaluation of the Copernicus Atmosphere Monitoring Service (CAMS) reanalysis against independent observations: Reactive gases. *Elementa: Science of the Anthropocene*, 9(1), 00171. https://doi.org/10.1525/elementa.2020.00171
- Wang, X., Wu, Y., Randel, W., & Tilmes, S. (2020). Stratospheric contribution to the summertime high surface ozone events over the western United States. *Environmental Research Letters*, 15(10), 1040a6. https://doi.org/10.1088/1748-9326/abba53
- Wargan, K., Labow, G., Frith, S., Pawson, S., Livesey, N., & Partyka, G. (2017). Evaluation of the ozone fields in NASA's MERRA-2 reanalysis. Journal of Climate, 30(8), 2961–2988. https://doi.org/10.1175/JCLI-D-16-0699.1
- Williams, R. S., Hegglin, M. I., Kerridge, B. J., Jöckel, P., Latter, B. G., & Plummer, D. A. (2019). Characterising the seasonal and geographical variability in tropospheric ozone, stratospheric influence and recent changes. Atmospheric Chemistry and Physics, 19(6), 3589–3620. https://doi.org/10.5194/acp-19-3589-2019
- Zanis, P., Hadjinicolaou, P., Pozzer, A., Tyrlis, E., Dafka, S., Mihalopoulos, N., & Lelieveld, J. (2014). Summertime free-tropospheric ozone pool over the eastern Mediterranean/Middle East. Atmospheric Chemistry and Physics, 14(1), 115–132. https://doi.org/10.5194/acp-14-115-2014
- Zhuang, J., Jacob, D. J., & Eastham, S. D. (2018). The importance of vertical resolution in the free troposphere for modeling intercontinental plumes. *Atmospheric Chemistry and Physics*, 18(8), 6039–6055. https://doi.org/10.5194/acp-18-6039-2018

BARTUSEK ET AL. 11 of 11